IOP Publishing Superconductor Science and Technology
Supercond. Sci. Technol. **28** (2015) 095016 (5pp) doi:10.1088/0953-2048/28/9/095016

$Ta_{1-x}Hf_xB$: a new FeB-prototype superconductor

A J S Machado[1], L E Corrêa[1], M S da Luz[1,2], F B Santos[1], B S de Lima[1], S T Renosto[1], O V Cigarroa[1], M R Custódio[1], C A Nunes[1], G C Coelho[1], P F Rogl[3], P F S Rosa[4], D J Kim[4] and Z Fisk[4]

[1] Escola de Engenharia de Lorena–USP, P. O. Box 116, Lorena, 12602-810, Brazil
[2] Universidade Federal do Triângulo Mineiro, Rua Dr Randolfo Borges Júnior 1250, Uberaba, 38066-200, Brazil
[3] Institute of Physical Chemistry, University of Vienna, Wahringerstrasse 42, A-1090 Wien, Austria
[4] Department of Physics and Astronomy, University of California-Irvine, Irvine, CA 92697, USA

E-mail: daluz.mario@icte.uftm.edu.br

Received 16 April 2015, revised 9 July 2015
Accepted for publication 12 July 2015
Published 11 August 2015

Abstract

In this work, we report superconductivity in the new ternary $Ta_{1-x}Hf_xB$ system. We also show clearly evidence that appropriate amounts of Hf substitution at the Ta site induce the stabilization of the orthorhombic FeB prototype structure in this system. Bulk superconductivity is confirmed by magnetization, electronic transport and specific heat measurements. The Hall signal has temperature dependence and the specific heat data at low temperature deviate from the conventional exponential temperature dependence in $Ta_{0.7}Hf_{0.3}B$. These results suggest multiband superconductivity in this compound.

Keywords: superconductivity, TaB system, two band superconductivity

(Some figures may appear in colour only in the online journal)

1. Introduction

The Ta–B binary system (Okamoto *et al* [1]) presents five stoichiometric phases, TaB_2, Ta_3B_4, TaB, Ta_3B_2 and Ta_2B. These well-known high temperature materials have special applications under extreme environmental conditions [2, 3]. In addition, recent investigations on the Ta rich side of this system suggest the existence of a new unidentified high-temperature phase [4]. Although these materials have been extensively studied, we can find only a few results on superconductivity in this system. Superconductivity has been reported for TaB and Ta_2B with critical temperatures of 4.0 and 3.12 K, respectively [5–7].

Here, we report the effect of Hf doping in the TaB system. TaB crystallizes in the orthorhombic CrB prototype structure (*Cmcm* space group) with lattice parameters $a = 3.27$ Å, $b = 8.66$ Å, and $c = 3.15$ Å [8]. We show clearly evidence that appropriate amounts of Hf substitution at the Ta site induce the stabilization of the FeB prototype structure in the ternary $Ta_{1-x}Hf_xB$ system. Superconductivity appears in these alloys with a maximum T_c (~6.7 K) for the $Ta_{0.7}Hf_{0.3}B$ compound. For this composition, the Hall signal has a temperature dependence which can be related to more than one electron velocity on the Fermi surface and the specific heat at low temperature deviates from the conventional exponential temperature dependence. These results are not expected at low fields within single-band BCS theory.

Multiband superconductivity has been observed in some superconducting materials such as MgB_2 and YNi_2B_2C [9–13]. In fact, MgB_2 is the clearest example and the most studied multiband superconductor. It has been confirmed by experimental techniques, such as high-resolution angle-resolved photoemission spectroscopy (ARPES) [9] and directional point-contact spectroscopy [10]. Based on these studies, our results suggest that the $Ta_{0.7}Hf_{0.3}B$ compound is a new multiband superconducting boride.

2. Experimental procedure

Polycrystalline samples of $Ta_{1-x}Hf_xB$ with $0 \leqslant x \leqslant 0.45$ were synthesized by arc melting. Stoichiometric amounts of

high purity elements Ta, Hf, and B were melted on a water cooled Cu hearth in an arc-furnace in an Ar atmosphere using a Ti sponge getter. The samples were flipped and re-melted 5 times to ensure good homogeneity. The weight loss during the arc melting was negligible (<0.3%). After melting, the samples were sealed in a special furnace and treated at 2000 °C for 8 h under an argon atmosphere. Powder x-ray diffraction (XRD) patterns were obtained using a Rigaku MultiFlex diffractometer which provides Cu K_α radiation. The lattice parameters were determined by using the PowderCell software and simulation as well [14].

Physical properties were investigated using a commercial VSM-PPMS EverCool II and also a VSM-SQUID magnetometer both from Quantum Design. Magnetization as a function of temperature was determined using zero field cooling (ZFC) and field cooling (FC) regimes, under an applied magnetic field of 20 Oe. In order to estimate the lower critical field, M versus H was measured from 1.8 to 6 K. Electrical resistivity as a function of temperature was measured using the standard four-probe method from 1.8 to 300 K. These measurements were performed both without and in an applied magnetic field in order to estimate the upper critical field. The specific heat of a polished flat sample with $Ta_{0.7}Hf_{0.3}B$ composition was measured in the range of 0.45–20 K using a He^3 system.

Here, we define the superconducting transition temperature (T_C) as the temperature corresponding to a 2% resistivity drop, a 1% magnetization drop in the ZFC measurements and a 1% heat capacity anomaly start from normal state.

To measure the Hall voltage, the sample was cut into a square with ∼4 mm sides and ∼0.5 mm thickness. The electrical contacts were placed on the corners of the sample. Low resistance contacts (∼0.1 Ω) were prepared by sputtering gold. Magneto-transport properties measurements were carried out in a in a commercial VSM-PPMS EverCool II with a 9 T magnet by using an adapted van der Pauw method with permutation of the voltage and current contacts (details about these measurements can be found in reference [15]).

3. Results and discussion

X-ray diffraction patterns for melted samples of $Ta_{1-x}Hf_xB$ with x up to 0.05 (not shown here) present the coexistence of diffraction peaks arising from two different orthorhombic symmetries. Most of the peaks can be indexed using the CrB prototype which is related to the TaB phase, and some peaks are also related to the FeB prototype (space group Pnma). We can also observe that the intensities of the diffraction peaks related to the TaB phase with the CrB prototype structure decrease with increasing Hf level. As x reaches values bigger than 0.05, only peaks associated with FeB symmetry remain and are still stable up to $x = 0.40$. These results indicate unambiguously that increasing the doped Hf concentration in $Ta_{1-x}Hf_xB$ can stabilize the orthorhombic FeB prototype structure in this system. Figure 1 shows a comparison between a simulated and experimental diffraction pattern for a polycrystalline sample of $Ta_{0.7}Hf_{0.3}B$.

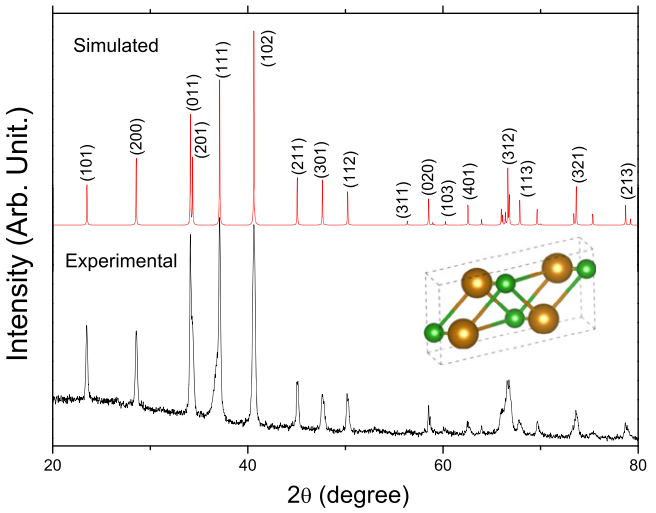

Figure 1. Comparison between simulated and experimental XRD for a polycrystalline sample of $Ta_{0.7}Hf_{0.3}B$. The inset shows a schematic view of the FeB prototype structure, where green spheres represent B atoms and yellow spheres Ta or Hf atoms.

The excellent agreement between experiment and simulation strongly suggests that Hf substitution in $Ta_{1-x}Hf_xB$ can stabilize the FeB prototype structure in this system. Rietveld refinement indicates lattice parameters equal to $a = 6.2462$ Å, $b = 3.1513$ Å and $c = 4.7496$ Å, at this substitution level. In this prototype structure, B occupies 4c at (0.13, 0.25, 0.3) and Ta/Hf share 4c at (0.325, 0.25, 0.615). The inset shows a schematic view of the crystal structure where the yellow spheres represent Ta or Hf atoms and the green spheres represent B atoms. Based on these results, we can say that Hf can stabilize a new boride compound not reported in the literature so far.

Excellent agreement between experimental and simulated FeB structure was also observed for compositions between $0.1 \leqslant x \leqslant 0.4$. In samples with x higher than 0.4, secondary phases can be observed coexisting with the FeB type structure, which indicates that $x = 0.4$ is the solubility limit for Hf substitution at the Ta site. In the $0.05 \leqslant x \leqslant 0.4$ range $Ta_{1-x}Hf_xB$ can be interpreted as a ternary compound.

It is well known that TaB binary compounds, with a CrB type structure, show superconductivity below ∼4.0 K [5]. When 10% of Ta atoms are replaced by Hf the FeB prototype structure is stabilized and the superconducting critical temperature goes up to 5.7 K, as verified by magnetization measurements. T_C increases as the Hf content increases and reaches a maximum close to the $Ta_{0.7}Hf_{0.3}B$ composition. A summary of our magnetization measurements is present in figure 2(a) which shows T_C as a function of Hf level (x–T_C phase diagram). We can clearly see a dome behavior with a maximum T_C close to $x = 0.30$. Thus, we will concentrate our discussion on this composition. Figure 2(b) shows a sharp superconducting transition close to 6.7 K for a sample of $Ta_{0.7}Hf_{0.3}B$. The inset shows M versus H at 1.8 K, displaying type II superconductivity. The shield observed in the Meissner state allows us to estimate a superconducting volume close to 55%, since the susceptibility value for perfect

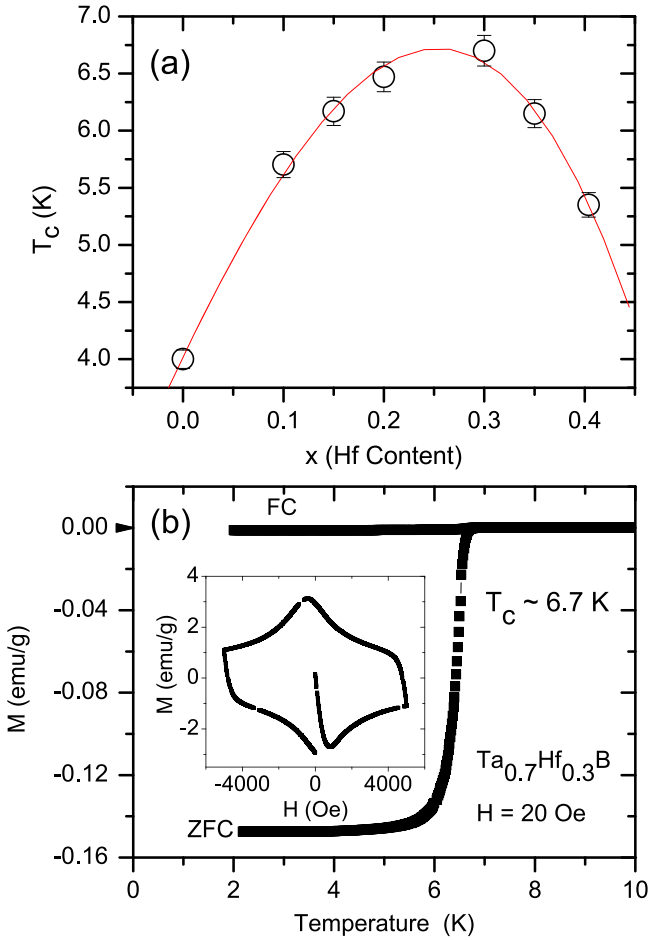

Figure 2. (a) T_C as a function of Hf content displaying a dome with maximum T_C close to $x = 0.30$. The red line is a guide to the eye. (b) M versus T for a polycrystalline sample of $Ta_{0.7}Hf_{0.3}B$ showing a superconducting transition close to 6.7 K. The inset shows the M versus H dependence at 1.8 K which suggests type II superconductivity.

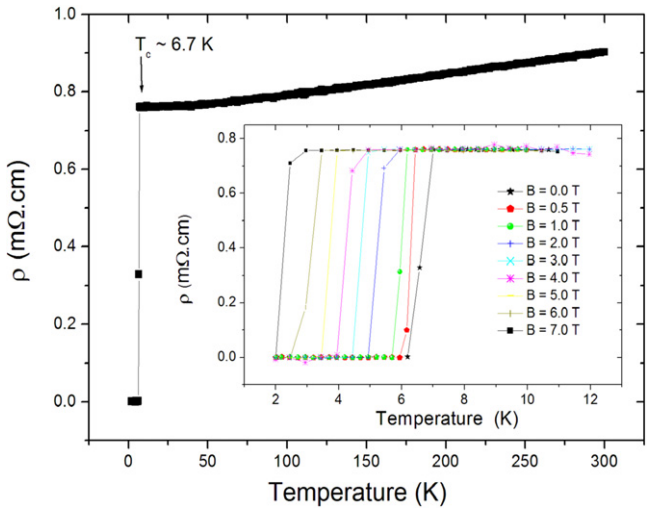

Figure 3. Resistivity versus T for the polycrystalline sample of $Ta_{0.7}Hf_{0.3}B$, showing the sharp transition with onset temperature close to 6.9 K. The inset shows ρ(B) versus T where the onset temperature transitions shift with applied magnetic field, as expected for a superconducting state.

diamagnetism is $-1/4\pi$ (CGS system). These results strongly suggest bulk superconductivity in this new boride material with $Ta_{0.7}Hf_{0.3}B$ composition.

Figure 3 shows resistivity as a function of temperature at zero magnetic field for a $Ta_{0.7}Hf_{0.3}B$ polycrystalline sample. The sharp transition reflects the good quality of our sample. The onset of the superconducting transition is estimated to be 6.7 K and zero resistivity is reached at 6.2 K. This 0.5 K difference shows very good agreement with the magnetization measurements shown in figure 2(b). This can be explained by a high density of defects caused by the quenching procedure at high temperature and also the distortion in the lattice due to the chemical doping. The residual resistivity ratio value, RRR = 1.3, supports this explanation.

The inset of figure 3 displays the dependence of the superconducting critical temperature on the applied magnetic field, showing a shift of the critical temperature typical of superconducting behavior. The magnetoresistance behavior suggests a relatively high upper critical field ($\mu_0 H_{c2}$). A $\mu_0 H_{c2}$–T phase diagram was constructed using a criterion of

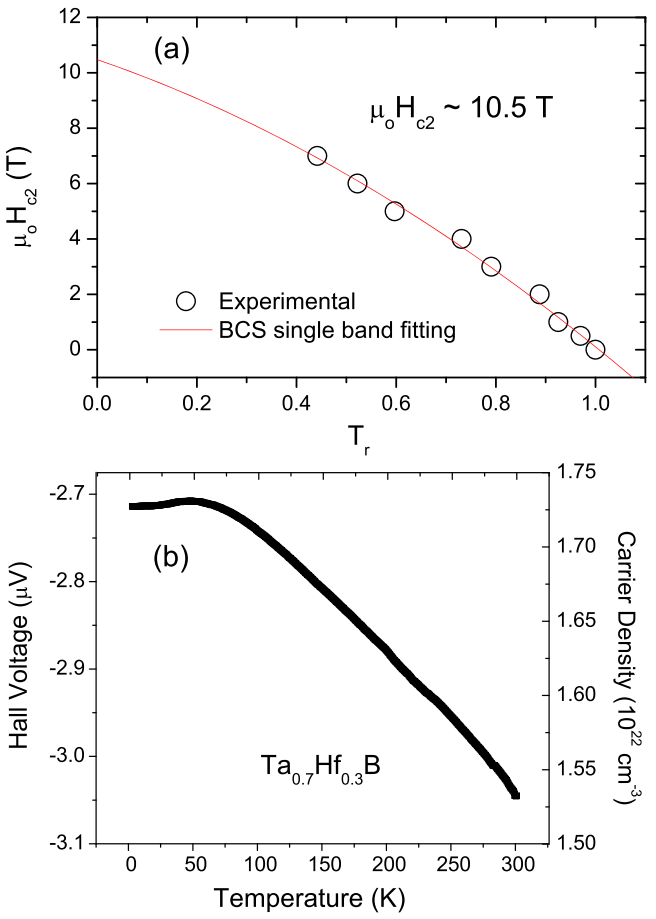

Figure 4. (a) $\mu_o H_{c2}(0)$ versus temperature (black symbols). The red line is the fit estimated by WHH theory [16]. The error bars are smaller than the symbols. (b) Hall voltage as a function of temperature at an applied magnetic field of 7.0 T (left axis). Carrier density is of order 10^{22} cm^{-3} suggesting that electrons are the majority carrier (right axis).

50% of normal state resistance, as shown in figure 4(a). The upper critical field at zero temperature ($\mu_o H_{c2}(0)$) can be estimated using the Werthamer–Helfand–Hohenberg (WHH) formula [16] in the limit of short electronic mean-free path (dirty limit),

$$\mu_o H_c(0) = -0.693 T_c \left(\mathrm{d}\mu_o H_c/\mathrm{d}T\right)_{T=Tc}. \quad (1)$$

The curve estimated by the WHH formula allows us to determine a $\mu_o H_{c2}(0)$ value of ~10.5 T (see red line in figure 4(a)). This value is consistent with resistivity measurements where zero resistance can be observed even at a 7.0 T applied magnetic field (see figure 3).

Focusing on the normal state properties of $Ta_{0.7}Hf_{0.3}B$, figure 4(b) shows Hall voltage as a function of temperature. The Hall signal has a temperature dependence which can be related to more than one electron velocity on the Fermi surface, suggesting two different scattering times. According to this theory [17], the longitudinal conductivity is governed by the transport scattering time t proportional to $1/T$, while the Hall conductivity follows $1/T^3$ since the Hall relaxation rate is proportional to $1/T^2$. In fact, this behavior is also observed in MgB_2 thin films which are recognized as classical multiband compounds [18, 19]. The carrier density of 10^{22} cm^{-3} in $Ta_{0.7}Hf_{0.3}B$ suggests a relatively high density of states at the Fermi level. The voltage signal suggests that the majority carriers are electrons.

Finally, specific heat measurements are shown in figure 5(a) for $Ta_{0.7}Hf_{0.3}B$. A jump (anomaly) in C_p/T versus T appears close to 6.7 K as we found from resistivity and magnetization measurements (figures 2 and 3). The sharp specific heat anomaly indicates bulk superconducting behavior, consistent with the superconducting volume estimated from magnetization measurements. As expected, below T_C the specific heat signal must decrease exponentially and reaches zero at zero Kelvin, according to thermodynamic predictions. In spite of this, our results show that the specific heat has a finite saturation at low temperature in C_p/T versus T (figure 5(a)).

In order to separate the phononic contribution, we have used the Debye approximation at low temperature given by $C_p/T = \gamma + \beta T^2$, which yields $\gamma = 2.0$ mJ mol^{-1} K^{-2} and $\beta = 0.11\,222$ (mJ mol^{-1} K^{-4}). Using the β value we can calculate a Debye temperature $\Theta_D \sim 325.93$ K. Subtracting the phonon contribution allows us to evaluate separately the electronic contribution to the specific-heat, plotted as C_e/T versus T in figure 5(b). An analysis of the jump yields $\Delta C_e/\gamma_n T_c \sim 1.11$ which is somewhat close to the BCS prediction (1.43), indicating that this gap is in the weak-coupling limit. Surprisingly, an unexpected upturn emerges at $T* \sim 1.4$ K in the C_e/T versus T data. In fact, similar behavior has been reported and attributed to either Schottky contributions or magnetic impurities [20, 21]. However, $Ta_{0.7}Hf_{0.3}B$ has no Schottky contributions and also has no magnetic impurities. Thus, this unexpected upturn may relate to a second superconducting gap and can be explained using the multiband scenario. Based on this, our results suggest that the $Ta_{0.7}Hf_{0.3}B$ compound is a new multiband superconducting boride, but further measurements at lower temperatures should be performed to look for the signature of a second gap.

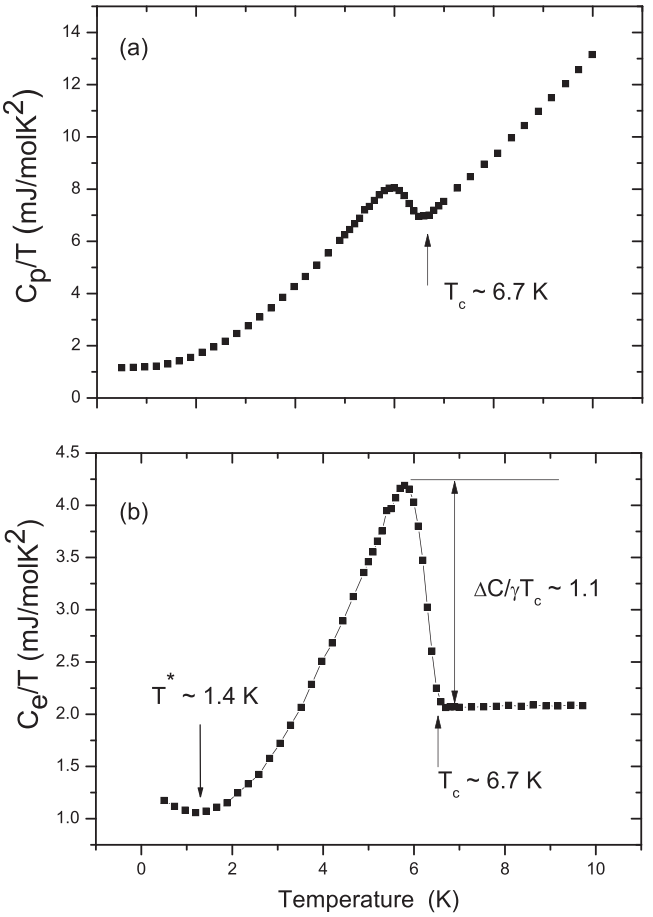

Figure 5. (a) C_p/T versus T showing the superconducting anomaly at ~6.7 K. (b) Electronic contribution to specific heat which reveals that the $\Delta C/\gamma T_c$ value is close to the BCS prediction (1.43).

4. Conclusion

In this paper, the physical properties of a new superconducting ternary system $Ta_{1-x}Hf_xB$ were explored. We show that substitution of Ta by Hf ions can stabilize the orthorhombic FeB prototype structure in these compounds. Superconductivity arises in this system with a maximum $T_c \sim 6.7$ K near the composition $Ta_{0.7}Hf_{0.3}B$. The heat capacity data deviate from conventional BCS theory, which could indicate some unconventional superconducting behavior in this material, possibly related to multiband effects in $Ta_{0.7}Hf_{0.3}B$. Additionally, the Hall constant has strong temperature dependence, similar to that seen in multiband MgB_2, suggesting that this compound is a new example of a multiband superconducting boride.

Acknowledgments

This material is based upon work supported by the FAPESP (2011/05961-3, 2014/01581-0, 2013/20181-0), NAP-USP, FAPEMIG, CNPq (448041/2014-6, 300821/2012-3) and CAPES (CAPES/CNPq PVE A10/2013), to which the authors wish to express their thanks.

References

[1] Okamoto H 1993 *J. Phase Equilib.* **14** 393–4
[2] Fahrenholtz W G and Hilmas G E 2012 *Int. Mater. Rev.* **57** 61–72
[3] Xuanru R, Hejun L, Qiangang F and Kezhi L 2014 *Ceram. Int.* **40** 9419–25
[4] Chad V M, Trindade Ramos E C, Coelho G C, Nunes C A, Suzuki P A, Ferreira F and Rogl P 2006 *J. Phase Equilib. Diffus.* **27** 452–5
[5] Shulishova O L and Shcherback I A 1967 *Inorg. Mater.* **3** 1304–6
[6] Savitskii E M, Baron V V, Efimov Y V, Bychkova M I and Myzenkova L F 1973 *Superconducting Materials* (New York: Plenum)
[7] Buzea C and Yamashita T 2001 *Supercond. Sci. Technol.* **14** R115–46
[8] Kiessling R 1949 *Acta Chem. Scand.* **3** 603
[9] Tsuda S, Yokoya T, Takano Y, Kito H, Matsushita A, Yin F, Itoh J, Harima H and Shin S 2003 *Phys. Rev. Lett.* **91** 127001–127001
[10] Gonnelli R S, Daghero D, Ummarino G A, Stepanov V A, Jun J, Kazakov S M and Karpinski J 2002 *Phys. Rev. Lett.* **89** 247004
[11] Mukhopadhyay S, Sheet G, Raychaudhuri P and Takeya H 2005 *Phys. Rev.* B **72** 014545
[12] Suderow H, Tissen V G, Brison J P, Martínez J L, Vieira S, Lejay P, Lee S and Tajima S 2004 *Phys. Rev.* B **70** 134518
[13] Shulga S V, Drechsler S-L, Fuchs G, Müller K-H, Winzer K, Heinecke M and Krug K 1998 *Phys. Rev. Lett.* **80** 1730–3
[14] Kraus W and Nolze G 1996 *J. Appl. Cryst.* **29** 301–3
[15] da Luz M S, de Carvalho F J H Jr, dos Santos C A M, Shigue C Y, Machado A J S and Ricardo da Silva R 2005 *Physica* C **419** 71–8
[16] Werthamer N R, Helfand E and Hohenberg P C 1966 *Phys. Rev.* **147** 295
[17] Yang H *et al* 2008 *Phys. Rev. Lett.* **101** 67001
[18] Masui T and Tajima S 2003 *Physica* C **385** 91–7
[19] Xi X X 2008 *Rep. Prog. Phys.* **71** 116501
[20] Wang Y, Plackowski T and Junod A 2001 *Physica* C **355** 179–93
[21] Fisher R A, Gordon J E, Hardy F, Mickelson W E, Oeschler N, Phillips N E and Zettl A 2013 *Physica* C **485** 168–76